Journal of Umm Al-Qura University for Applied Science 7 (1), (2021) 12-15

Journal of Umm Al-Qura University
for Applied Science

journal homepage: https://uqu.edu.sa/en/jas/87823

Effects of reducing the free volume in the intercalated bilayers of tricarbosilane liquid crystalline dimers and monomers

Sarah Hosawi [a], Carsten Müller [b], Frank Giesselmann [b], Robert P. Lemieux [a *].

[a] *Chemistry Department, Queen's University, Kingston, Ontario, Canada.*
[b] *Institute of Physical Chemistry, Universitat Stuttgart, Pfa ¨ fenwaldring 55, D-70569 Stuttgart, German.*

ARTICLE INFO

Article History:
Submission date: 29-1-2021
Accepted date: 25-5-2021

Keywords:
liquid crystals, Smectic, dimers.

ABSTRACT

Smectic liquid crystals with a low layer contraction of less than 1% upon an SmA to SmC transition are referred to as 'de Vries-like'. These materials have attracted considerable attention as possible alternative to problems with surface-stabilized ferroelectric liquid crystals in liquid crystal displays. The 'de Vries-like' properties of liquid crystals with nanosegregating carbosilane segments are enhanced by lengthening the carbosilane end-groups from mono- to tricarbosilane. The observed enhancement is thought to arise from an increase in the cross-section of the free volume in the hydrocarbon sub-layer. The hypothesis is tested by assuming that dimers with a tricarbosilane linking group have smaller time-averaged cross-sections. This paper reports the synthesis and characterization of two homologous series of liquid crystals and an investigation of their mesogenic properties as model systems employing liquid crystalline monomers ***(QL39-n)*** *and dimers* ***(QL40-n)*** *comprising 2-phenylpyrimidine cores and tricarbosilane end-groups and spacers, respectively. We find that the* ***QL39-n*** *monomers form only a tilted SmC phase, whereas the* ***QL40-n*** *dimer forms an orthogonal SmA phase due to the tricarbosilane spacer will not have a spherically shape on the time average like that predicted for the tricarbosilane end-group. Results are discussed in the context of the time-averaged cross-sections of the materials.*

1. Introduction

Liquid crystal dimers have long been used as model compounds for semi-flexible main-chain liquid crystal polymers1. Here, the term dimer refers to particles that have two rigid mesogenic units connected by a flexible spacer such as an alkyl chain. The calamitic mesogens of the liquid crystal have two phases: nematic (N) and smectic (SmC or SmA) (Fig. 1).

Researchers often elect to study liquid crystals comprising chemically inert carbosilane rather than hydrolytically labile organosiloxane end groups, because the former materials are more suitable for liquid crystal displays2. New liquid crystal mesogenic structures comprising a mixture of SmC-promoting and SmA-promoting elements have been developed in recent years2,3. The model mesogen, QL6-6 3, has a carbosilane end group, which supports the upright nanosegregated character of a SmC phase that is fundamental to liquid crystal formation. QL6-6 also contains a chloro-terminated alkyl group, which is a SmA-promoting element. Mesogen QL-16-6 4 has a carbosilane end group that promotes the SmC phase and a 5-phenylpyrimidine core as the SmA-promoting element. The two materials experience a SmA–SmC transition with a layer contraction of 0.4–0.5%.

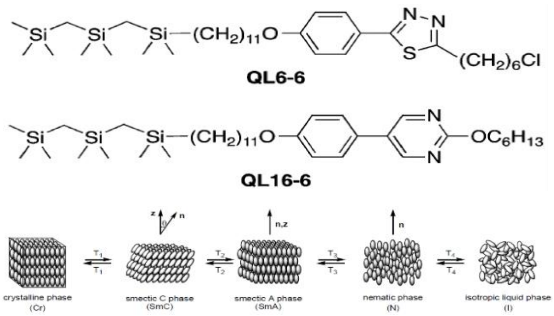

Figure 1. Scheme of phase transitions between crystalline, smectic C, smectic A, nematic (N), and isotropic liquid phases for a calamitic material as a function of temperature.

We have synthesized the tricarbosilane **QL13-n**, dicarbosilane **QL18-n**, and monocarbosilane **QL19-n** [5] to study the relationship between 'de Vries-like' properties and the length of the carbosilane end-group. Achievement of 'de Vries-like' behavior[6,7] in materials is realized through nanosegregation[8], which is important for creating high lamellar ordering[9,10]. Low orientational order also is important in establishing 'de Vries-like' behavior. The results show an increase in nanosegregation in the carbosilane end group and a decrease in orientational order upon increasing the length of the end group from mono- to tricarbosilane. This work pursues a greater understanding of this behavior.

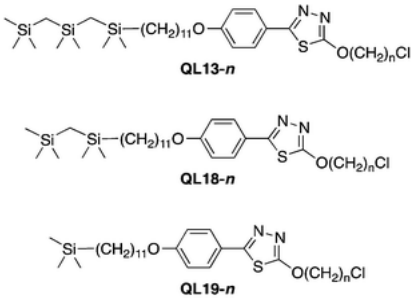

We assume from our recent study on the effect of carbosilane nanosegregation on 'de Vries-like' properties that the tricarbosilane end group is approximately spherical in shape owing to its shallow torsional energy profiles[4]. Carbosilane-terminated mesogens form an intercalated bilayer structure allowing nanosegregation to produce "backfilling."[10] A significant fraction of free volume in the hydrocarbon sub-layer may lead to an increase in the orientational fluctuations that minimize free energy [5]. Figure 2 illustrates the decrease in orientational fluctuation of the mono- and dicarbosilane end groups due to their smaller size relative to that of tricarbosilane. Herein, we examine the hypothesis that the size of the carbosilane end group modulates orientational free by investigating the mesogenic properties of the model tricarbosilane dimers, **QL40-*n***, containing a 2-phenylpyridine core in comparison with those of the mesogenic

* **Corresponding Author**
Department of Chemistry, Faculty of Applied Sciences, Umm Al-Qura University, Makkah, Saudi Arabia.
E-mail address: **rplemieux@uwaterloo.ca** (Robert P. Lemieux).

monomers, **QL39-*n***. The ultimate objective is to understand the origin of 'de Vries-like' behavior in carbosilane-terminated mesogens. The **QL39-*n*** is monomers series and **QL40-*n*** is dimers series.

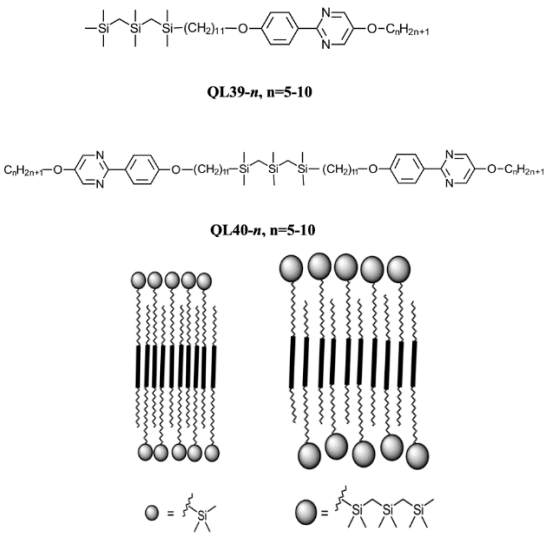

Figure 2. Schematic representations of the bulky size of the monocarbosilane (left) and tricarbosilane (right) end-groups.

2. Results and Discussion

2.1. Synthesis

Synthesis of the **QL39-*n*** monomers was accomplished by selective alkylation of commercially available 2-(4-hydroxyphenyl)pyrimidin-5-ol (**1**) with the appropriate alcohol via a Mitsunobu reaction. A mixture of 2-(4-hydroxyphenyl)pyrimidin-5-ol, alcohol, and triphenylphosphine (PPh3) in dry tetrahydrofuran (THF) was added dropwise to diisopropyl azodicarboxylate (DIAD) at room temperature. After stirring for 24 h, the solvent was removed under reduced pressure, and the solid residue was purified by column chromatography on silica gel to give **2-*n*** (Scheme 1)[11]. A second alkylation with 1-bromo-12,12,14,14,16,16-hexamethyl-12,14,16-trisilaheptadecane afforded **QL39-*n***. Alternatively, alkylation of **2-*n*** with 10-undecen-1-ol via a Mitsunobu reaction afforded **3-*n*,** which was converted to **QL39-*n*** via a platinum-catalyzed hydrosilation reaction using 1,1,1,3,3,5,5-heptamethyltrisilane and Karstedt's catalyst[12]. Synthesis of the dimeric **QL40-*n*** series was carried out by alkylation of **2-*n*** with 1,27-dibromo-12,12,14,14,16,16-hexamethyl-12,14,16-trisilaheptacosane in methyl ethyl ketone as shown in Scheme 2[11]. The monomer and dimer compounds were recrystallized from ethanol.

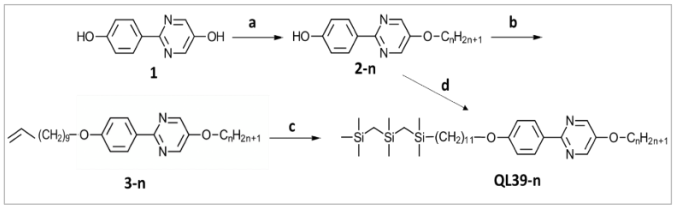

Scheme 1. Reagents and conditions: (a) CnH2n+1OH, DIAD,PPh3, and THF at room temperature overnight or CnH2n+1Br K2CO3 and methyl ethyl ketone at reflux, overnight; (b) C11H21OH, DIAD, PPh3, and THF at room temperature overnight; (c) 1,1,1,3,3,5,5-heptamethyltrisilane, Karstedt's catalyst, and toluene for 48 h; (d) 1- bromo-12,12,14,14,16,16-hexamethyl-12,14,16-trisilaheptadecane, K2CO3, and methyl ethyl ketone.

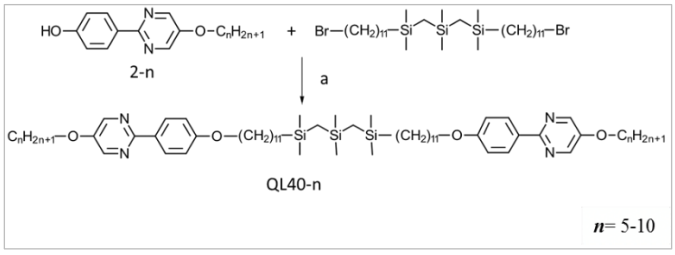

Scheme 2. Reagents and conditions: (a) K2CO3 and methyl ethyl ketone at reflux, overnight.

2.2. Mesophase characterization

The mesophases formed by **QL39-*n*** monomers and **QL40-*n*** dimers were characterized by polarized optical microscopy (POM) and differential scanning calorimetry (DSC) analyses were performed on a TA Instruments Q2000 instrument with scanning rate of 5 K min-1. All monomeric mesogens in the series n = 5–10 form the SmC phase upon heating and cooling, as shown by the appearance of a low-birefringence gray Schlieren texture (Fig. 3). The dimers form a SmA phase upon cooling from the isotropic liquid, as shown by characteristic fan textures and dark homeotropic domains (Fig. 4a). We also observed significant changes in the **QL40-5**, **QL40-6, QL40-7**, and **QL40-8** dimers at temperatures below formation of the SmA phase**,** where the dark homeotropic domains transform into a gray texture. This property shows that the phase is tilted, although no broken fans are observed (Fig. 4b). The alterations are accompanied by a change in the interference colors resulting from a change in birefringence. The unidentified phase is denoted as the SmX phase. This modification in behavior, which is not detected by DSC (Fig. 3) due to the impossibility of measuring the optical tilt angles (θopt)[13] by POM, may be due to an unusual layer contraction of the dimer structure as confirmed by the X-ray scattering results. These experiments and the electro-optic response analysis indicate that the SmX phase does not behave like an SmC phase. In addition, the SmA phase is not observed for the monomeric series, which suggests that the properties of the dimer and monomer are noticeably different.

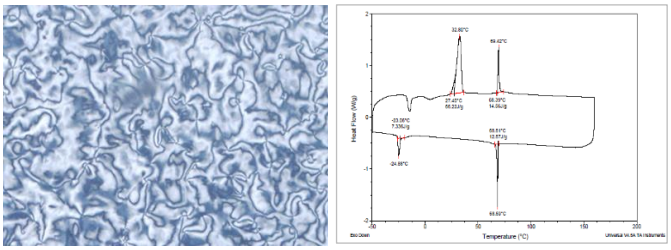

(a) (b)

Figure 3. (**a**) Polarized photomicrograph of **QL39-6** monomer on cooling showing the SmC phase at 70°C; (**b**) DSC profile of **QL39-6** at 5 K/min scan rate.

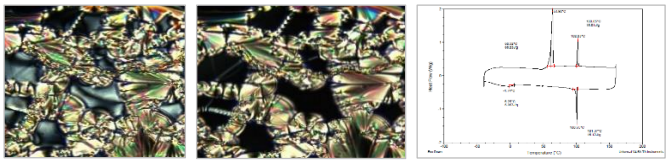

(a) (b) (c)

Figure 4. Polarized photomicrographs of the **QL40-6** dimer on cooling: **(a)** SmA phase at 91 °C and **(b)** SmX phase at 74 °C; (**C**) DSC profile of **QL40-6** at 5 K/min scan rate.

Phase transition by temperatures in °C

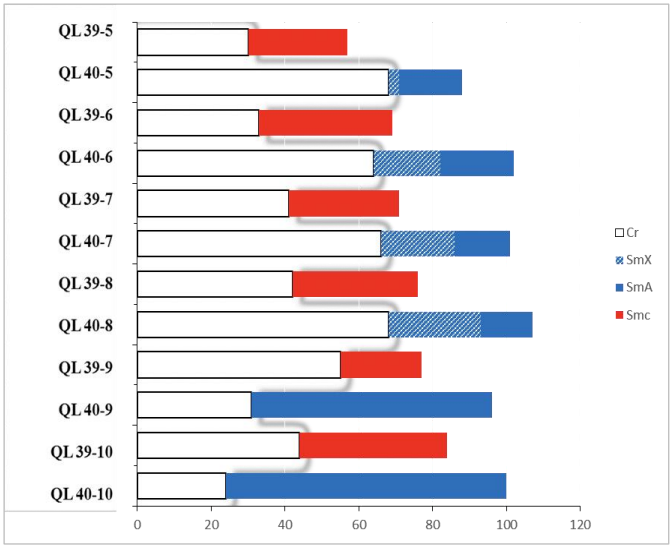

Figure 5. Phase transition temperatures (°C) of **QL39-*n*** monomers and **QL40-*n*** dimers determined by DSC upon heating at 5 K/min rate.

Figure 5 shows that the temperature ranges of the SmC and SmA phases formed by monomers and dimers, respectively, tend to be similar for C6–C8, narrower for C5, and broader for C10. The uniform temperature range of the SmX phase in **QL40-*6*** through **QL40-*8*** is approximately 21 K. The **QL40-*n*** dimers exhibit a larger increase in

their melting point relative to the corresponding monomers apart from the C9 and C10 dimers, for which the melting points decrease by 24 and 20 K, respectively (Fig. 5). The progression from monomer to dimer generally produces a significant increase in the clearing point, which corresponds to an increase in the stability of the smectic layer14. The enthalpies of the monomers and dimers listed in Table 1 demonstrate that the enthalpy changes for both series of compounds are consistent with a first-order process for the crystalline–smectic and smectic–isotropic transitions.

Table 1. Transition temperatures (°C) and enthalpies of transition (kJ /mol, in parentheses) for **QL39- *n*** and **QL40- *n*** compounds.

Compounds	Cr	SmX	SmA	SmC	I
QL 39-5	• 30 (40)			• 57 (7)	•
QL 39-6	• 33 (43)			• 69 (9)	•
QL 39-7	• 41 (49)			• 71 (8)	•
QL 39-8	• 42 (43)			• 77 (10)	•
QL 39-9	• 55 (59)			• 77 (8)	•
QL 39-10	• 44 (41)			• 84 (11)	•
QL 40-5	• 68 (79)	•72	•88 (11)		•
QL 40-6	• 64 (72)	•85	•102 (15)		•
QL 40-7	• 66 (74)	•88	•101 (16)		•
QL 40-8	• 68 (66)	•93	•107 (14)		•
QL 40-9	• 31 (46)		•96 (12)		•
QL 40-10	• 24 (40)		• 100 (19)		•

2.3. X-ray scattering experiments

The layer spacing, *d*, was measured by small-angle X-ray scattering (SAXS) and mono-domain 2D X-ray scattering as a function of temperature. The X-ray scattering was recorded with a CCD detector (KAF 2084x2083 SCX) and processed and analysed using the SAXSquant 3.5 software for the **QL40-6** dimer using SAXS in accordance with Bragg's equation:

$$n\lambda = 2d\sin\theta$$

The method is advantageous for investigating the structure of smectic phases formed by dimeric mesogens. Figure 6 shows that *d* measured upon heating from the crystalline phase is effectively temperature invariant between 84 and 102 °C. The value of *d* decreases significantly at lower temperatures with a maximum layer contraction of 9%. The apparent transition point is identical to that of a SmA–SmX phase transition, for which the dark homeotropic domains transition into a gray texture under POM. The behavior is consistent with a conventional SmA–SmC transition. The *d*-values obtained by X-ray analysis of the SmA phase (42.5 Å) are less than the length of fully extended **QL40-6** (L = 73.3 Å) calculated according to the model at 3D Optimization (ACDLABS/3D) . The ratio of d/L = 0.57 suggests that the molecules in the SmA phase have an intercalated bilayer arrangement [15]. This configuration is a typical result of mixing the two patterns, which shows the distinctive X-ray diffraction (XRD) features of the SmA phase at 70 and 100 °C. The X-ray patterns exhibit a characteristic layered structure that manifests as a sharp Bragg reflection along the layer normal, **z**, in the small-angle region. These features are consistent with smectic layering.

Diffuse wide-angle scattering also is observed along the axis orthogonal to z, which corresponds to the intermolecular distance between the hydrocarbon and carbosilane segments1,15. Analysis via 2D X-ray scattering of a mono-domain shows no azimuthal rotation of the wide-angle versus small-angle reflection at the apparent SmA–SmX transition point (Fig. 7).

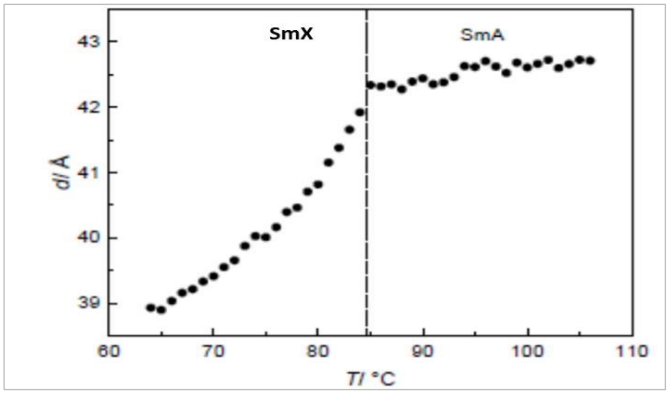

Figure 6. Smectic layer spacing, *d*, versus reduced temperature, $T - Tx$, for **QL40-6**.

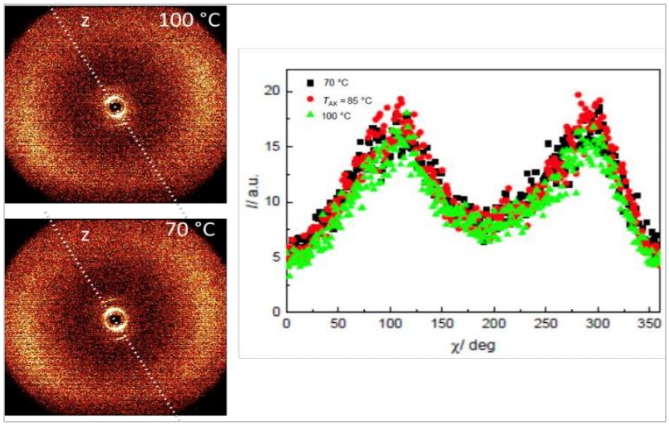

Fig. 7. 2D X-ray scattering patterns at $T - TAX$ = +15 K and $T - TAX$ = -10 K (left), and diffuse wide-angle scattering as function of azimuthal angle χ for **QL40-6** at 70, 85, and 100 °C (right).

2.4. Electro-Optic Response

Accurate measurement of the electro-optic behavior of the mesophases formed by the **QL39-6** and **QL40-6** monomers was conducted at 5 mol% doping with the chiral dopant, **QL32-6**16. The results confirm that the **QL40-6** dimer does not form a tilted smectic or an anticlinic phase. The doped **QL39-6** sample, which forms only a SmC* phase, exhibits good alignment with contrasting dark and light textural domains[17,18,19]. Figure 8a shows that application of a triangular AC voltage across the film produces a polarization current reversal consisting of one peak in each direction, which is characteristic of the ferroelectric ground state of a SmC* phase. However, the doped **QL40-6** sample aligned under the same conditions does not respond to a triangular-wave voltage across the film in either the high-temperature SmA* or low-temperature SmX* phase. **QL40-6** also fails to exhibit a polarization current reversal or evidence of switching behavior under POM (Fig. 8b). The electro-optical response behavior and the results of the X-ray measurements confirm that the SmX mesophase formed by the **QL40-6** dimer is neither a synclinic (SmC_c) nor an anticlinic (SmCa) phase. We note that antiferroelectric ordering has been observed in organosiloxane liquid crystals and attributed to molecular conformation[20].

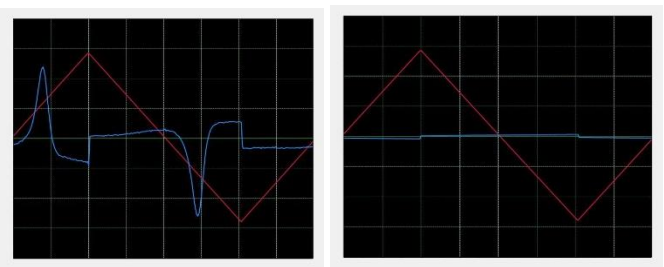

(a) **(b)**

Figure 8. Polarization current reversal profiles for for 4-μm surface-stabilized films of (a) **QL39-6** and (b) **QL40-6** (in the SmX phase) doped with the chiral mesogen **QL32-6** (5 mol%) upon application of a triangular AC voltage of 6 V/μm and 100 Hz.

The ultimate difference between the two models is that the system incorporating a tricarbosilane spacer does not adopt the time-averaged spherical shape expected for a tricarbosilane end group. This difference occurs because the molecules are aligned perpendicular to the layers with the two mesogenic units extending in opposite directions along the **z**-axis (system uniaxiality20), which results in a more extended configuration of the tricarbosilane spacers. This property is illustrated in Fig. 9. Therefore, a tricarbosilane spacer will have a smaller time-averaged cross-section. We note that the small cross-section of a monocarbosilane end group provides a lower degree of nanosegregation than does a tricarbosilane end-group, which decreases the degree of SmC-promotion in the carbosilane unit and explains why **QL40-*n*** forms a SmA rather than SmC phase[21]. In a SmX phase, the contraction of *d* with decreasing temperature may result from an increase in the core-core interactions that drive an increase in intercalation.

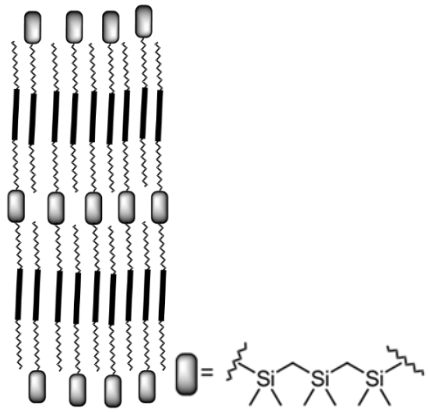

Figure 9. Schematic representation of the bulky character of the tricarbosilane unit in the SmA dimer phase.

3. Conclusions

Two new families of carbosilane liquid crystal dimers and monomers were synthesized by alkylation of a 2-phenylpyrimidine scaffold and tricarbosilane spacers and end-groups. The dimers and monomers exhibit distinct mesomorphic properties, which may rise from a difference in flexibility of the tricarbosilane units in a lamellar organization. The **QL39-n** monomers form only a tilted SmC phase, whereas the **QL40-n** dimers form an orthogonal SmA phase and a lower-temperature SmX phase. The SmX phase exhibits some characteristics of the SmC phase including a birefringent Schlieren texture and a contraction of the layer spacing. However, 2D X-ray scattering and electro-optical response experiments strongly suggest that SmX is an orthogonal phase with an atypical layer contraction in the dimer structure. The transition from monomer to dimer is accompanied by an expansion of the clearing point, which may reflect a dissimilarity in the degree of nanosegregation of the monomers and dimers, as well as a difference in the strength of the van der Waals interactions between core structures. This behavior is consistent with our hypothesis that the tricarbosilane spacer in **QL40-*n*** has a smaller time-averaged cross section than the monomer. The reason for the decrease in the **QL40-*n*** layer spacing upon the SmA–SmX transition remains unclear, although a possible explanation is that the layer contraction is due to an increase in the degree of interdigitation.

References

[1] Demus, D.; Goodby, J.; Gray, G. W.; Spiess, H. W.; Vill, V. Handbook of Liquid Crystals, Volume 7: Liquid Crystal Dimers and Oligomers, 1998.
[2] Song, Q.; Nonnenmacher, D.; Giesselmann, F.; Lemieux, R. P. *J. Mater. Chem. C* **2013**, *1*, 343.
[3] Song, Q.; Bogner, A.; Giesselmann, F.; Lemieux, R. P. *Chem. Commun.* **2013**, 49, 8202.
[4] Mulligan, K. M.; Bogner, A.; Song, Q.; Shubert, P. J.; Giesselmann, F.; Lemieux, R. P. *J. Mater. Chem. C* **2014**, *2*, 8270.
[5] Schubert, C. P.; Bogner, A.; Porada, J. H.; Ayub, K.; Andrea, T.; Giesselmann, F.; Lemieux, R. P. *J. Mater. Chem. C* **2014**, *2*, 4581.
[6] De Vries, A. *Mol. Cryst. Liq. Cryst.* **1977**, *41*, 27.
[7] De Vries, A. *J. Chem. Phys.* **1979**, *70*, 2705.
[8] Tschierske, C. *J. Mater. Chem.* **1998,** *8*, 1485.
[9] Lagerwall, J. P. F.; Giesselmann, F. *ChemPhysChem* **2006**, *7*, 20.
[10] Shoosmith, D.; Carboni, C.; Perkins, S.; *Mol. Cryst. Liq. Cryst. Sci. Technol., Sect. A.* **1999**, *331*, 2041.
[11] Sarah, H. Characterization of New Carnosine Liquid Crystalline Monomers and Dimers under supervisor Robert P. Lemieux. https://qspace.library.queensu.ca/handle/1974/14717.
[12] Zhang, Y.; O'Callaghan, M. J.; Walker, C.; Baumeister, U.; Tschierske, C. Chem. Mater. 2010, 22, 2869.
[13] McMillan, W. L. Phys. Rev. A 1973, 8 , 1921.
[14] Dunmur, D. *Liquid Crystal Fandmantals*; *Physical Properties of Liquid Crystal*, 2002.
[15] Imrie, C. T.; Henderson, P. A. *Chem. Soc. Rev.*, **2007**, *36*, 2096.
[16] Schubert, C. P.; Müller, C.; Wand, M. D.; Giesselmann, F.; Lemieux, R. P. *Chem. Commun.*, **2015**, 51.
[17] Kuczynski, W.; Stegemeyer, H. *Chem. Phys. Lett.* **1980**, *70*, 123-126.
[18] Handschy, M. A.; Clark, N. A.; *Appl. Phys. Lett.* 1982, 41, 39.
[19] Meyer, R. B.; Liebert, L.; Strzelecki, L.; Keller, P. J. Phys. (Paris), Lett. 1975, 36, L69- L71.
[20] Robinson, W. K.; Carboni, C.; Kloess, P.; Perkins, S. P.; Coles, H. J. *Liq. Cryst.*, **1998**, *25*, 301.
[21] Mulligan, K. M.; Bogner, A.; Song, Q.; Shubert, P. J.; Giesselmann, F.; Lemieux, R. P. *J. Mater. Chem. C* **2014**, *2*, 8270.